Soft X-Ray Resonant Diffraction Study of Magnetic and Orbital Correlations in a Manganite Near Half Doping

K. J. Thomas,[1] J. P. Hill,[1] S. Grenier,[1,2] Y-J. Kim,[1] P. Abbamonte,[3] L. Venema,[4] A. Rusydi,[3] Y. Tomioka,[5] Y. Tokura,[5,6] D. F. McMorrow,[7] G. Sawatzky,[8] and M. van Veenendaal[9]

[1]*Department of Physics, Brookhaven National Laboratory, Upton, New York 11973, USA*
[2]*Department of Physics and Astronomy, Rutgers University, Piscataway, New Jersey 08854, USA*
[3]*National Synchrotron Light Source, Brookhaven National Laboratory, Upton, New York 11973, USA*
[4]*Materials Science Centre, University of Groningen, 9747 AG Groningen, The Netherlands*
[5]*Correlated Electron Research Center (CERC), National Institute of Advanced Industrial Science and Technology (AIST), Tsukuba 305-8562, Japan*
[6]*Department of Applied Physics, University of Tokyo, Tokyo 113-8656, and Spin Superstructure Project, ERATO, Japan Science and Technology Corporation (JST), Tsukuba 305-8562, Japan*
[7]*London Centre for Nanotechnology and Department of Physics and Astronomy, University College London, London WC1E 6BT, United Kingdom*
[8]*University of British Colombia, Vancouver, British Colombia, Canada V6T 1Z4*
[9]*Northern Illinois University, Dekalb, Illinois 60115, USA, and Argonne National Laboratory, Argonne, Illinois 60439, USA*

We have utilized resonant x-ray diffraction at the Mn $L_{II,III}$ edges in order to directly compare magnetic and orbital correlations in $Pr_{0.6}Ca_{0.4}MnO_3$. Comparing the widths of the magnetic and orbital diffraction peaks, we find that the magnetic correlation length exceeds that of the orbital order by nearly a factor of 2. Furthermore, we observe a large (~ 3 eV) spectral weight shift between the magnetic and orbital resonant line shapes, which cannot be explained within the classic Goodenough picture of a charge-ordered ground state. To explain the shift, we calculate the orbital and magnetic resonant diffraction line shapes based on a relaxed charge-ordered model.

In the manganites, the dynamics resulting in a charge-ordered, insulating ground state in the vicinity of half doping are still not well understood. In his seminal work on exchange interactions in manganites, Goodenough considered charge and orbital order as a precursor to the antiferromagnetic ground state observed in half-doped manganites [1]. In this picture, charge ordering at T_{CO} results in a checkerboard pattern of Mn^{3+} and Mn^{4+} sites (Fig. 1). The Mn^{3+} sites each have one e_g electron and are thus Jahn-Teller (JT) active, while the e_g levels are empty on the Mn^{4+} sites. A cooperative JT distortion and orbital ordering of the Mn^{3+} sites occurs at $T_{OO} = T_{CO}$, concomitant with the charge ordering. The in-plane JT distortions favor occupation of $3x^2$-r^2 and $3y^2$-r^2 orbitals on the Mn^{3+} sites, establishing a ferromagnetic exchange pathway along orbital zigzag chains (dotted line, Fig. 1). Magnetic ordering, defined by antiferromagnetically coupled ferromagnetic chains, occurs at $T_N \leq T_{OO}$.

Extensive neutron and x-ray scattering measurements support the Goodenough picture [2–6]. However, this model makes definite predictions about the Mn ground state for which experimental confirmation is still lacking. One controversial issue is the degree to which the "Mn^{3+}" and "Mn^{4+}" sites are actually separated by unit valence. Indeed, a number of experimental results challenge the charge ordering model [7,8]. Recent analysis of Mn K-edge resonant x-ray diffraction in

$Pr_{0.6}Ca_{0.4}MnO_3$ suggests that the charge ordering is far from complete, but supports the presence of an orbitally ordered ground state [9]. In addition, the Goodenough model predicts a strong coupling between the orbital and magnetic correlations within the Mn^{3+} sublattice. However, no single experimental technique has been able to directly compare magnetic and orbital correlations.

Recent experiments have demonstrated the resonant enhancement of magnetic and orbital diffraction in manganites at the Mn L edges [10–12]. The Mn $L_{II,III}$ edge resonances involve strong dipole transitions from the $2p$ core levels to unoccupied states within the $3d$ band, providing not only an enormous enhancement of the
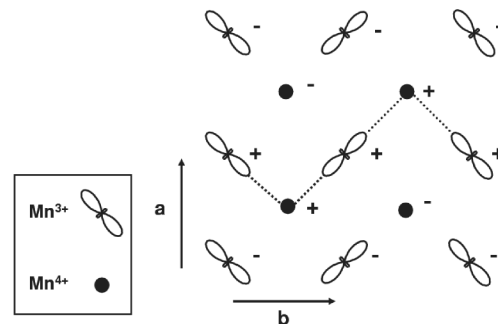

FIG. 1. Magnetic ground state for half-doped manganites. The plus and minus signs denote spin directions.

magnetic scattering but a direct probe of the Mn $3d$ states in the presence of correlations [13].

In this Letter, we present a resonant x-ray diffraction study of a near half-doped manganite at the Mn $L_{II,III}$ edges which permits the first direct comparison between magnetic and orbital correlations. Our data provide evidence against a charge ordering into distinct Mn^{3+} and Mn^{4+} sublattices, and indicate a more complex ground state. First, we find that the magnetic correlations are significantly longer ranged than the orbital correlations. Second, the spectral line shapes and the difference in intensity between the magnetic and orbital scattering disagree with the ionic, charge-ordered picture. Rather, we suggest that, while the e_g electron is still localized, it is shared between neighboring lattice sites [14].

We have focused on a twinned, single crystal of $Pr_{0.6}Ca_{0.4}MnO_3$, which has been described as a charge and orbital ordered antiferromagnet, as shown in Fig. 1, with $T_{OO} = T_{CO} \sim 240$ K and $T_N \sim 170$ K [3]. The orbital and spin orderings result in superlattice reflections at $(0, \frac{1}{2}, 0)$ and $(\frac{1}{2}, 0, 0)$, respectively, based on an orthorhombic unit cell ($a = 5.41$ Å and $b = 5.43$ Å). The twinned crystal has both [100] and [010] oriented domains at the sample surface such that both $(\frac{1}{2}, 0, 0)$ and $(0, \frac{1}{2}, 0)$ reflections are accessible at nearly the same scattering angles ($2\theta \sim 124°$). Although these reflections are not resolved in momentum space, the magnetic and orbital scattering are clearly distinguished by different transition temperatures and correlation lengths.

The diffraction measurements were performed at the National Synchrotron Light Source X1B undulator beam line. The spectrometer is housed in a UHV chamber to reduce adsorption on the sample surface. Slits before and after the grating monochromator determined the energy resolution, which was <1 eV (calculated). The incident beam was π polarized and the crystal c axis was oriented normal to the scattering plane.

Measurements of the energy dependent resonant diffraction are performed by sitting at fixed $\mathbf{Q} = (\frac{1}{2}, 0, 0)/(0, \frac{1}{2}, 0)$ and scanning through the Mn L_{III} ($2p_{3/2} \rightarrow 3d$) and L_{II} ($2p_{1/2} \rightarrow 3d$) absorption edges. Figure 2(a) shows energy scans taken at 183 K, below T_{OO} but above T_N, and at 100 K, below T_N. An energy scan at 240 K has been subtracted from both spectra to remove the contribution from specular reflectivity and fluorescence. To emphasize the difference in the line shapes, the two curves are scaled to the same intensity at their respective maxima. As we discuss below, the peak in the 100 K spectrum ($\sim 60\,000$ counts/s) is actually 100 times more intense than that of the 183 K spectrum.

In addition to the large change in intensity, there is a dramatic shift in the resonant spectral weight upon warming through T_N: Below T_N there is a sharp peak at 645.5 eV within the L_{III} region and smaller scattering within the L_{II}. Above T_N, the peak in the L_{III} occurs at 648.5 eV and the L_{III} and L_{II} scattering are nearly equal in intensity. Within the two temperature regions, $T < T_N$ and
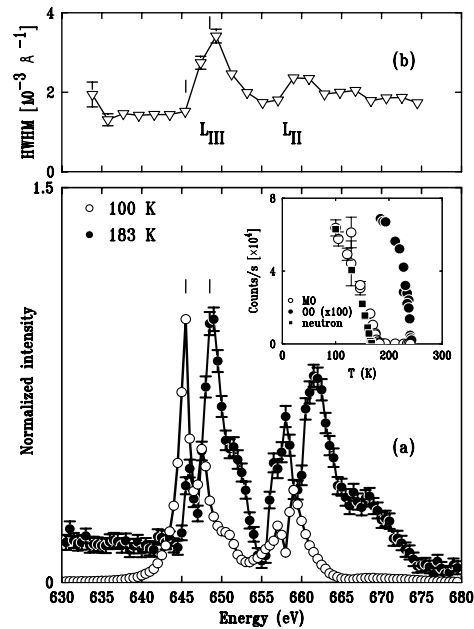

FIG. 2. (a) Energy scans at a fixed wave vector at 100 K ($T < T_N$) and 183 K ($T_N < T < T_{OO}$). (Inset) Temperature dependence of the peaks in the magnetic (MO, open circles) and orbital (OO, closed circles) spectra and the $(\frac{3}{2}, 0, 0)$ magnetic reflection measured with neutrons (dark squares). (b) HWHM of the $(\frac{1}{2}, 0, 0)$ magnetic peak versus energy, indicating the increase in absorption at the Mn L edges. The tick marks denote the peaks in the magnetic and orbital spectra.

$T_N < T < T_{OO}$, the line shape remains constant, exhibiting an order-parameter-like dropoff in intensity first around 175 K and then at 240 K. This suggests that, below T_N, the spectrum is dominated by magnetic scattering while, above T_N, the spectrum is pure orbital scattering. The inset of Fig. 2(a) shows the temperature dependence of the intensities measured at 645.5 and 648.5 eV, the peak energies in the magnetic and orbital spectra, respectively. (The intensity of the 648.5 eV feature is indicated only above 180 K, as the contribution from the magnetic scattering dominates at lower temperatures.) The transition temperatures, $T_N = 175$ K and $T_{OO} = 240$ K, agree well with those measured in Ref. [3], and comparison with neutron data on the same sample [15] confirms that the intensity below T_N is indeed sensitive to the magnetic ordering.

Figure 2(b) shows the HWHM of the magnetic Bragg peak versus energy. Away from the $L_{II,III}$ edges, photoelectric absorption limits the penetration depth to ~ 1000 Å. Figure 2(b) indicates the further decrease in penetration depth as the incident energy is tuned through the edges, resulting in a broadening of the peak. Comparing Figs. 2(a) and 2(b) shows that the peak in the absorption coincides with the peak in the orbital spectrum. We note that the spectra in 2(a) are not corrected for absorption; however, calculations of the absorption suggest that it does not significantly affect the line shapes.

This study permits the first direct comparison of magnetic and orbital correlations in a manganite. Figure 3 shows longitudinal momentum scans through the orbital and magnetic diffraction peaks at 645 eV. This energy is just below the absorption edge, permitting greater experimental resolution compared to higher energies. Defining the inverse correlation length, $\frac{1}{\xi}$, to equal the HWHM obtained from a fit to a Lorentzian line shape, we find an orbital correlation length $\xi_b^{\mathrm{orb}} = 370 \pm 30$ Å. The magnetic correlation length is nearly a factor of 2 longer with $\xi_a^{\mathrm{mag}} = 720 \pm 30$ Å. (We find a similar discrepancy between magnetic and orbital correlation lengths in transverse scans.) We note that the orbital peak is significantly broader than the magnetic peak at all energies, indicating that the difference in widths results from intrinsic differences in the two correlation lengths and not from absorption or extinction effects.

Although the magnetic and orbital correlation lengths were determined at different temperatures, in fact we have confirmed that the orbital correlation length does not change below T_N. We measured the orbital and magnetic scattering with the c axis in the scattering plane [16]. In this geometry, the two intensities were comparable and the orbital scattering could be observed above and below T_N. We found that the orbital diffraction peak width remained broad below T_N.

Short-ranged orbital correlations with $\xi_b^{\mathrm{orb}} \sim 320$ Å were also found in K edge resonance experiments in $Pr_{0.6}Ca_{0.4}MnO_3$ [17]. Neutron scattering measurements showed similarly short-ranged magnetic correlations in the Mn^{3+} sublattice, leading to the suggestion that the Mn^{3+} magnetic and orbital correlation lengths were identical [3,17]. These results supported the Goodenough model, since in this picture orbital domain walls create magnetic domain walls in the Mn^{3+} sublattice. In the ground state shown in Fig. 1, the diffraction at $(\frac{1}{2}, 0, 0)$ and $(0, \frac{1}{2}, 0)$ is sensitive only to the Mn^{3+} sites. We clearly find longer range correlations between spins than orbitals
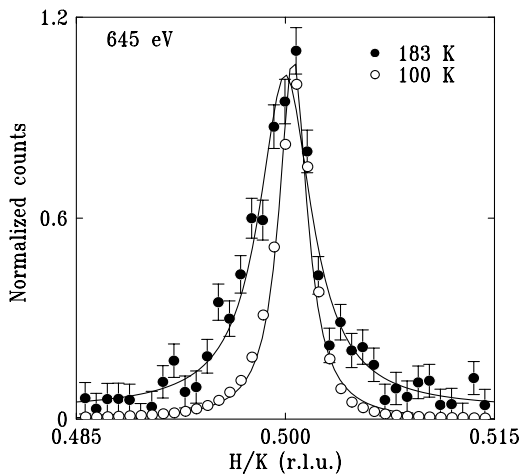

FIG. 3. Longitudinal momentum scans above ($T = 183$ K) and below ($T = 100$ K) T_N at 645 eV.

within this sublattice, which directly challenges the Goodenough picture of magnetic and orbital coupling.

Two further challenges to the single ion picture of the Goodenough model lie in the comparison between the magnetic and orbital resonant line shapes and intensities. First, the orbital line shape peaks at energies where there is little spectral weight in the magnetic scattering. This is difficult to reconcile with a single atom picture, for which the spectral weight of the magnetic and orbital scattering is expected to lie in the same energy range. Second, the magnetic scattering is significantly stronger than the orbital scattering. Since a larger population of a- and b-oriented domains could favor magnetic scattering, we performed an experiment in which we optimized the beam position on the sample surface separately for the orbital and magnetic spectra. We found the ratio of magnetic to orbital peak intensities was closer to $\sim$25:1. Other factors will also contribute to a smaller orbital scattering, such as the shorter in-plane correlation length and greater absorption at the orbital peak energy.

However, we find we can describe both the resonant line shapes and difference in intensities by assuming a more realistic ground state in which the e_g electron is shared between neighboring sites,

$$|g\rangle = \alpha|3;4\rangle + \beta|4;3\rangle. \tag{1}$$

Here, $|i;j\rangle$ denotes i electrons on a JT distorted site (where the scattering takes place) and j electrons on a neighboring site along a ferromagnetic chain. (In the ionic model, $|g\rangle = |4;3\rangle$.) The hopping parameter t that couples the two configurations in Eq. (1) is of order 1– 1.5 eV and significantly larger than the JT energy of 0.1– 0.3 eV. We can therefore expect $\alpha \cong \beta$.

The inclusion of coupling to a neighboring site leads to two different (dipole allowed) intermediate states:

$$|n_1\rangle = \alpha'|\underline{c}5;3\rangle + \beta'|\underline{c}4;4\rangle, \tag{2}$$

$$|n_2\rangle = \beta'|\underline{c}5;3\rangle - \alpha'|\underline{c}4;4\rangle, \tag{3}$$

where $\underline{c}$ denotes a $2p$ core hole. Within an ionic picture, the energy difference $\Delta_1 = E_{|\underline{c}5;3\rangle} - E_{|\underline{c}4;4\rangle}$ is related to the Coulomb interactions between $3d$ electrons, U_{dd}, and between the $3d$ electrons and the $2p$ core hole, U_{pd}. Thus, $\Delta_1 = U_{dd} - U_{pd}$, which can be of the order of a few eV. In the presence of finite hopping, t, the intermediate states are split by $\Delta_2 = E_{|n_2\rangle} - E_{|n_1\rangle} = (4t^2 + \Delta_1^2)^{1/2}$.

The ground-state configurations $|3;4\rangle$ and $|4;3\rangle$ make significantly different contributions to the orbital scattering. Contributions to orbital scattering occur in two ways. First, the JT distortions split the $3d$ intermediate states, leading to finite orbital scattering on resonance. This effect occurs for both intermediate state configurations $|\underline{c}4;4\rangle$ and $|\underline{c}5;3\rangle$. However, as shown in Ref. [18], this effect is important only if the JT splitting is significantly larger than the core-hole lifetime of 0.3–0.5 eV. A second and much stronger effect occurs if the lower e_g level on the JT site is occupied in the ground state, as is the case for the $|4;3\rangle$ configuration.
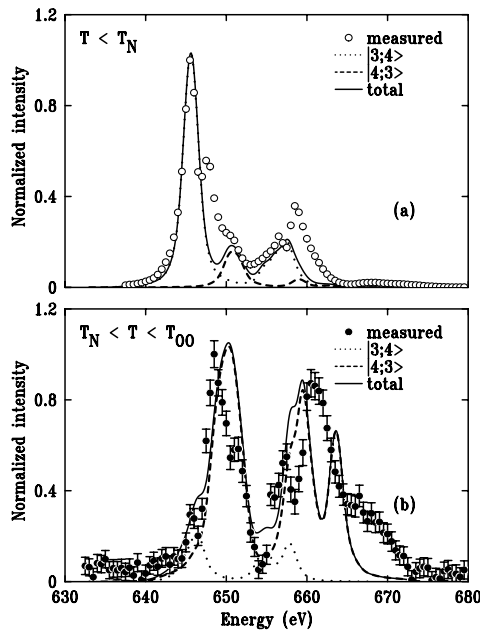
FIG. 4. Comparison between the calculated and measured resonance line shapes. In (a) the magnetic scattering is dominated by the $|3;4\rangle$ configuration while in (b) the orbital scattering is dominated by the $|4;3\rangle$ configuration.

In contrast, the magnetic scattering from the $|3;4\rangle$ and $|4;3\rangle$ configurations is not expected to differ strongly in intensity. It is, however, straightforward to show that the ratio of scattering intensities to intermediate state $|n_1\rangle$ compared to $|n_2\rangle$ is $r = [(\alpha\alpha' + \beta\beta')/(\alpha\alpha' - \beta\beta')]^4$. Assuming $\alpha \cong \beta$, $t = 1.1$ eV, and $\Delta_2 = 3.5$ eV, we obtain $\frac{\alpha'}{\beta'} = [\Delta_1 + (4t^2 + \Delta_1^2)^{1/2}]/(2t) = 2.8$ and $r = 19.6$. This shows that the scattering through $|n_1\rangle$ is about 20 times stronger than through $|n_2\rangle$ and dominates the magnetic scattering. Similarly, the orbital scattering arising from $|n_2\rangle$ will be significantly smaller than the magnetic scattering from $|n_1\rangle$.

To quantify these arguments, we calculated the magnetic and orbital scattering in the ordered state by exact diagonalization of a Hamiltonian including the full U_{pd} and U_{dd} interactions and the $2p$ and $3d$ spin-orbit coupling for the different configurations. We assumed an octahedral crystal field of 1.5 eV and a 0.1 eV JT splitting of the e_g orbitals. The calculated spectra were convolved with a 1 eV (FWHM) Lorentzian and a 1 eV (FWHM) Gaussian to account for lifetime and experimental broadening, respectively.

The results are compared with the measured spectra in Fig. 4, which shows the separate and combined contributions from the $|3;4\rangle$ and $|4;3\rangle$ configurations. Figure 4(a) shows the magnetic scattering, which is dominated by the $|3;4\rangle$ configuration. The $|4;3\rangle$ contribution is strongly reduced by the spectral weight effect described above. Figure 4(b) shows the orbital spectrum. It is dominated by the $|4;3\rangle$ configuration which, though reduced by the same spectral weight transfer compared to the magnetic

scattering, still contributes more strongly than the $|3;4\rangle$ configuration to the orbital scattering.

We note that this model is preliminary and that a number of open questions remain. For example, the model cannot explain why the magnetic spectrum is strongest below the peak in the absorption, or the broad feature at 668 eV in the orbital spectrum. This broad feature appears to be particular to the orbital scattering and has been observed in several recent reports [11,12]. Nevertheless, we feel the model is a step in the right direction and illustrates the quality of ground-state information obtained with this technique.

In summary, we have measured the resonant line shape at the Mn L edge in $Pr_{0.6}Ca_{0.4}MnO_3$, at $T_N < T < T_{OO}$ and at $T < T_N$. The comparison of the magnetic and orbital line shapes, in addition to theoretical calculations, strongly suggest that the Mn sites are highly mixed between the Mn^{3+} and Mn^{4+} formal oxidation states. Furthermore, we find that the magnetic correlations are longer ranged than the orbital correlations. These findings pose a direct challenge to the classic Goodenough picture of charge, orbital, and magnetic order in half-doped manganites. The results presented here emphasize the sensitivity of resonant diffraction at the Mn L edge to the ground state of the $3d$ electrons and encourage a new approach to theoretical calculations.

[1] J. B. Goodenough, Phys. Rev. **100**, 564 (1955).
[2] P. G. Radaelli et al., Phys. Rev. B **55**, 3015 (1997).
[3] Z. Jirák et al., J. Magn. Magn. Mater. **53**, 153 (1985).
[4] Y. Moritomo et al., Phys. Rev. B **51**, 3297 (1995).
[5] B. J. Sternlieb et al., Phys. Rev. Lett. **76**, 2169 (1996).
[6] M. v. Zimmermann et al., Phys. Rev. B **64**, 195133 (2001).
[7] J. García et al., J. Phys. Condens. Matter **13**, 3229 (2001).
[8] A. Daoud-Aladine et al., Phys. Rev. Lett. **89**, 097205 (2002).
[9] S. Grenier et al., Phys. Rev. B **69**, 134419 (2004).
[10] S. B. Wilkins et al., Phys. Rev. Lett. **90**, 187201 (2003).
[11] S. B. Wilkins et al., Phys. Rev. Lett. **91**, 167205 (2003).
[12] S. S. Dhesi et al., Phys. Rev. Lett. **92**, 56403 (2004).
[13] J. P. Hannon et al., Phys. Rev. Lett. **61**, 1245 (1988).
[14] M. v. Veenendaal and A. J. Fedro, Phys. Rev. B **59**, 15 056 (1999).
[15] Young-June Kim et al. (unpublished).
[16] K. J. Thomas et al. (unpublished).
[17] J. P. Hill et al., Appl. Phys. A **73**, 723 (2001).
[18] C. W. M. Castleton and M. Altarelli, Phys. Rev. B **62**, 1033 (2000).